Nonlinear stability limit in high β tokamaks

Robert G. Kleva and Parvez N. Guzdar
Institute for Plasma Research, University of Maryland, College Park, Maryland 20770

(Received 9 June 1999; accepted 14 December 1999)

Linearly unstable high β tokamak equilibria are shown to be nonlinearly stabilized by an axisymmetric flow containing both toroidal and poloidal components. As fingers of hot plasma produced by pressure driven ballooning instabilities start to convect out towards the bounding wall, an axisymmetric flow is self-consistently generated and opposes the growth of the fingers, maintaining confinement. However, as β increases the growth rate of the fingers increases until there is insufficient time for the developing axisymmetric flow to halt their rapid progress to the wall, and confinement is lost. The ultimate stability of a tokamak plasma is determined by a nonlinear stability limit in β. © *2000 American Institute of Physics.* [S1070-664X(00)00304-9]

I. INTRODUCTION

The most important limitation on the performance of tokamaks as fusion reactors is the limitation on the plasma pressure imposed by disruptions. Attempts to increase the ratio β of the plasma pressure to the magnetic field pressure beyond a limit β_c are thwarted by an abrupt, catastrophic loss of confinement.[1–3] To date, all attempts at an explanation of this stability limit in β have been based on linear stability theory. However, linear stability calculations can not account for the salient features of the disruptive loss of confinement. The inadequacy of linear stability theories is demonstrated by the observed time scale over which energy confinement is lost during disruptions. Thermal confinement is rapidly destroyed on a very short time scale of the order of 100–400 μs, and not on longer time scales—there are no major β disruptions that are less rapid.[3] The existence of a maximum thermal quench time is incompatible with any linear stability criterion since just above marginal linear stability one would expect to see more slowly growing modes that generate slower disruptions with quench times longer than 400 μs. But slower disruptions are not seen to occur. Furthermore, it is observed that tokamak discharges in the vicinity of β_c often experience minor β disruptions that exhibit the same characteristics as major β disruptions, but are less violent so that the plasma can recover without termination of the discharge.[3] Although the tokamak plasma is linearly unstable, the instabilities often have little impact on the discharge. These experimental observations demonstrate that the stability of tokamak plasmas is ultimately determined by nonlinear effects.

In this paper we present an investigation of the nonlinear stability of high β toroidal plasmas. High β toroidal equilibria are linearly unstable to ballooning modes that grow on the pressure gradient on the large R side of the torus, where R is the major radius of the torus. The three-dimensional vortices generated by the linearly unstable modes act to convect the hot central plasma out toward the wall at large R in hot plasma ''fingers.''[4] Our investigation of the nonlinear evolution of these modes demonstrates that: (1) There is a nonlinear stability limit in β below which confinement is maintained, even though the equilibrium is linearly unstable. (2) Linearly unstable equilibria at lower β do not suffer a disruptive loss of confinement because the relatively slowly growing linearly unstable modes are stabilized nonlinearly. (3) The growing modes are stabilized by a self-consistent axisymmetric flow, independent of the toroidal angle, that is generated nonlinearly. This self-generated flow opposes the growth of the hot plasma fingers toward the wall at large R, thereby maintaining confinement. (4) The self-generated axisymmetric flow contains both poloidal and toroidal components. The poloidal component of the flow is not a simple poloidal rotation, but instead consists of two vortices, one located above the midplane of the torus and the other below. (5) As β increases the growth rate of the hot plasma fingers becomes so rapid that there is not sufficient time for the axisymmetric flow to halt their motion before they strike the wall at large R, and global confinement is lost. (6) Our simulations provide a natural explanation of the time scale of the thermal quench during β limit disruptions. There are not any thermal quenches that are longer than 400 μs because the more slowly growing modes are stabilized nonlinearly. (7) Our simulations also provide a natural explanation for the variety of disruptions of various intensity from minor to major. The more slowly growing the modes, the less impact they have on confinement before they are stabilized.

The rest of this paper is organized as follows. The equations and the toroidal equilibrium are discussed in Sec. II. The numerical results in Sec. III demonstrate that linearly unstable modes can be nonlinearly stabilized by a self-generated axisymmetric flow. The characteristics of this flow are detailed. In Sec. IV we consider the effect of increasing β on nonlinear stability. We summarize and discuss our results in Sec. V.

II. EQUATIONS

Our simulations are based on the nonlinear resistive magnetohydrodynamic (MHD) equations for the magnetic field $\mathbf{B}$, the mass velocity $\mathbf{V}$, the temperature T, and the mass density ρ_m,

$$\partial \mathbf{B}/\partial t = \nabla \times (\mathbf{V} \times \mathbf{B}) + \eta \nabla^2 \mathbf{B}, \tag{1}$$

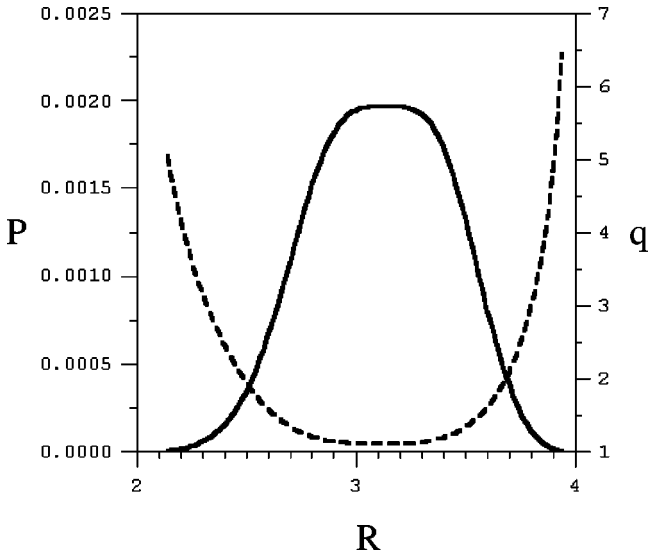

FIG. 1. Equilibrium. The pressure P (solid line) and the safety factor q (dashed line) are plotted vs the major radial coordinate R in the midplane ($z=0$), for an equilibrium with $\beta_{\mathrm{pol}}=0.3$.

$$\partial \mathbf{U}/\partial t+\nabla\cdot(\mathbf{VU})=\mathbf{J}\times\mathbf{B}-\nabla P+\mu\nabla^2\mathbf{U}, \tag{2}$$

$$\partial T/\partial t+\mathbf{V}\cdot\nabla T-\nabla_{\|}\kappa_{\|}\nabla_{\|}T=0, \tag{3}$$

$$\partial \rho_m/\partial t+\nabla\cdot\mathbf{U}-D\nabla^2\rho_m=0, \tag{4}$$

where the parallel gradient $\nabla_{\|}=\hat{\mathbf{b}}\cdot\nabla$ with $\hat{\mathbf{b}}=\mathbf{B}/|\mathbf{B}|$, the momentum density $\mathbf{U}=\rho_m\mathbf{V}$, the pressure $P=\rho_m T$, and the current $\mathbf{J}=\nabla\times\mathbf{B}$, for a plasma with resistivity η, viscosity μ, parallel thermal conductivity $\kappa_{\|}$, and diffusion coefficient D. Equations (1)–(4) are solved in toroidal geometry (R,ϕ,z), where R is the major radial coordinate of the torus, ϕ is the toroidal angle, and z is the vertical distance along the axis of the torus, with a square conducting wall of half-width a in the poloidal plane. The equations are given in normalized units[5] in which the time t is normalized to the Alfvén time $\tau_A\equiv a/v_A$ with v_A the Alfvén velocity, and the resistivity $\eta=S^{-1}$, where the Lundquist number $S\equiv\tau_r/\tau_A$ is the ratio of the resistive diffusion time τ_r to the Alfvén time. Let us consider equilibrium in a torus with aspect ratio $A\equiv R_0/a=3$, where R_0 is the major radius of the torus. An example of an axisymmetric equilibrium, independent of the toroidal angle ϕ, satisfying the force balance condition $\mathbf{J}\times\mathbf{B}=\nabla P$ is shown in Fig. 1. This figure is a plot of the pressure P and the safety factor q as a function of R through the midplane $z=0$. The ratio of the pressure P_0 at the magnetic axis to the square of the mean poloidal magnetic field is denoted by β_{pol},[5] while β_{tor} is defined as the ratio of P_0 to the square of the toroidal field $B_\phi(R=R_0)$. For the equilibrium in Fig. 1, $\beta_{\mathrm{pol}}=0.3$, $\beta_{\mathrm{tor}}=0.4\%$, and the central safety factor $q_0=1.1$. The equilibrium mass density is uniform in space. Equilibria with different β are obtained by changing the central pressure P_0. We have tested the ideal stability of these high pressure equilibria with a code that utilizes the ballooning approximation to solve the one-dimensional linear ballooning mode equation. The ideal stability limit is found to be at $\beta_{\mathrm{pol}}\approx 1$. With the inclusion of nonideal effects, the equilibria are unstable at lower β_{pol}. In the nonlinear simulations, the normalized transport coefficients are given by $\eta=\mu=D=3\times10^{-4}$. The ion pressure is the dominant source of instabilities in high β tokamaks since the bulk of the thermal energy resides in the ions. At the core of a large hot tokamak ($R_0=260$ cm, $a=80$ cm, $B_\phi=40$ kG, density $n=5\times10^{13}$ cm^{-3}, central temperature $T=10$ keV), the Alfvén time $\tau_A\approx 0.1\mu$s and the ion–ion collision time $\tau_{ii}\approx 20$ ms $\approx 2\times10^5\tau_A$. On time scales shorter than τ_{ii}, the ions are collisionless and stream freely down magnetic field lines. With a time-dependent parallel thermal coefficient $\kappa_{\|}=v_i{}^2t$, where v_i is the ion thermal velocity, the time scale $\tau_{\|}$ for the transport of energy a distance s down a magnetic field line is given by the free-streaming result $\tau_{\|}=s/v_i$.

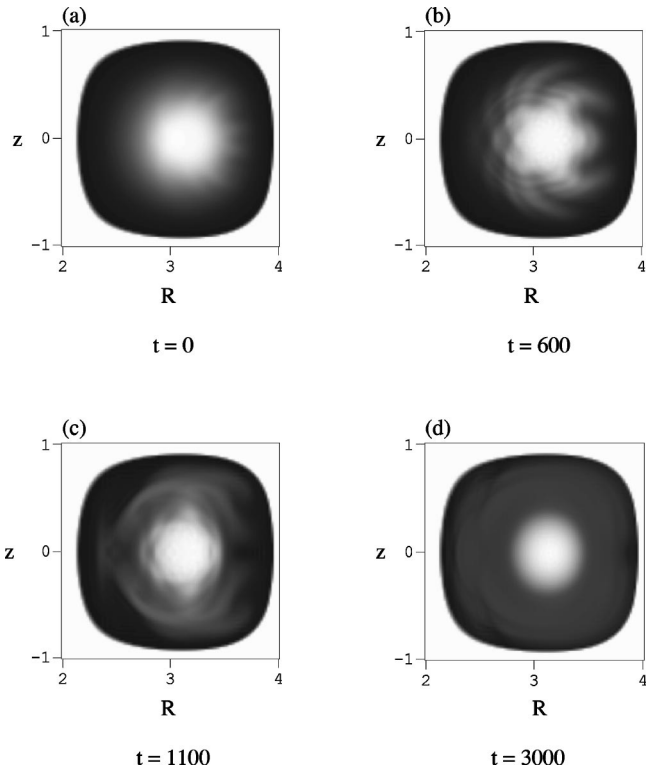

FIG. 2. Nonlinear evolution. The temporal evolution of the pressure is plotted in the poloidal plane (R,z) at $\phi=0$ for a plasma with $\beta_{\mathrm{pol}}=0.3$, at $t/\tau_A=$(a) 0, (b) 600, (c) 1100, and (d) 3000.

III. STABILIZATION BY AN AXISYMMETRIC FLOW

The nonlinear temporal evolution of a three-dimensional perturbation applied to the $\beta_{\mathrm{pol}}=0.3$ equilibrium of Fig. 1 is shown in Fig. 2. This figure is a plot of the pressure in the poloidal plane (R,z) at $\phi=0$, at four different times during the evolution. The lightly shaded areas near the center are the regions of hotter, high pressure plasma while the colder, low pressure plasma is located in the darker areas. In order to eliminate any possible influence of the hyperbolic X-points of the poloidal magnetic field at the four corners of the square, the plasma is surrounded by a wall located at the flux surface $\psi=0.1\psi_{\mathrm{axis}}$, where $\psi=\psi_{\mathrm{axis}}$ at the magnetic axis and $\psi=0$ at the square boundary. The white area in Fig. 2 surrounding the plasma column is outside this wall. The results of a simulation with the plasma bounded by the square wall

are similar to those shown in Fig. 2. At $t=0$ [Fig. 2(a)] the perturbation is small but growing because the free energy associated with the pressure gradient and the unfavorable magnetic curvature at large R destabilizes ballooning modes. By $t=600\tau_A$ [Fig. 2(b)] the plasma enters a nonlinear phase in which fingers of hot plasma are convecting out towards the wall at large R. But subsequently the growth of the fingers is blunted and the fingers are turned inwards toward the midplane ($z=0$) of the torus [Fig. 2(c)], away from the wall, and global confinement is maintained. The energy in the hot fingers is simultaneously spread along the magnetic field lines by parallel conduction, and the toroidal plasma reaches the stable quasi-equilibrium shown in Fig. 2(d). The pressure profile has been somewhat broadened as the low temperature edge plasma has been spread out into a halo around the high temperature core by the instabilities, but the energy in the hot plasma remains confined away from the wall. Once the plasma settles into the quasiequilibrium shown in Fig. 2(d), this state persists virtually unchanged.

The progress of the hot fingers toward the wall at large R is halted by an axisymmetric flow, independent of the toroidal angle ϕ, that is self-consistently generated as the fingers evolve nonlinearly. The structure of this axisymmetric flow is shown in Fig. 3. Figure 3(a) is a vector plot of the poloidal component of the flow $\langle \mathbf{V}_{\mathrm{pol}} \rangle_\phi$, where $\langle \cdot \rangle_\phi$ denotes an average over ϕ, in the poloidal plane (R,z) at $t=1100\tau_A$. The poloidal component of the axisymmetric flow consists of two vortices, one above the midplane $z=0$ of the torus and one below, that convect the growing hot fingers toward the midplane and then inward towards smaller R, and prevent the fingers from reaching the wall at large R. Figure 3(b) is a plot of the toroidal component of the flow $\langle V_\phi \rangle_\phi$ in the poloidal plane at the same time. The lighter areas are the regions in which the flow is in the positive ϕ direction, while the flow is in the negative ϕ direction in the darker areas. The axisymmetric toroidal flow is antisymmetric about the midplane $z=0$. Moving above the midplane away from the magnetic axis, the toroidal flow first increases in magnitude in the positive ϕ direction, but then reverses direction in ϕ. The temporal dependence of the axisymmetric flow is shown in Fig. 4(a), where the maximum value in the poloidal plane of both the poloidal and toroidal flow speed, normalized to v_A, is plotted. As the fingers grow, the self-generated flow increases in magnitude with time, reaching approximately $2\times10^{-4}v_A$ (0.2% of the sound speed c_s, since $c_s/v_A\approx0.1$) when $t=1100\tau_A$. After $1900\tau_A$, the magnitude of this flow saturates at less than 0.5% of c_s as the plasma relaxes into the quasiequilibrium shown in Fig. 2(d). The results in Figs. 2–4(a) are virtually unchanged when the Reynolds stress $\nabla\cdot(\mathbf{VU})$ is arbitrarily eliminated from the momentum Eq. (2). Thus, the axisymmetric flow is generated by the nonlinear pressure and magnetic forces, and not by the nonlinear Reynolds stress. The equilibrium pressure gradient at the midplane on the large R side of the magnetic axis produces a force on the plasma that is outward in R. In equilibrium, this outward pressure force is balanced by an inward Lorentz force caused by the compression of the poloidal magnetic field against the wall on the outboard side of the torus. The unstable ballooning modes preferentially transport energy in the large R direction thereby reducing the average pressure gradient at large R. Thus, the average outward pressure force is reduced in magnitude so that it is no longer large enough to completely balance the inward Lorentz force. The result is that there is now a small net inward force that generates the average axisymmetric flow as the compressed poloidal magnetic field relaxes slightly. In order to resolve the nonlinear gradients in the pressure and flows on the numerical grid, the magnitude of the dissipation coefficients η and μ in the

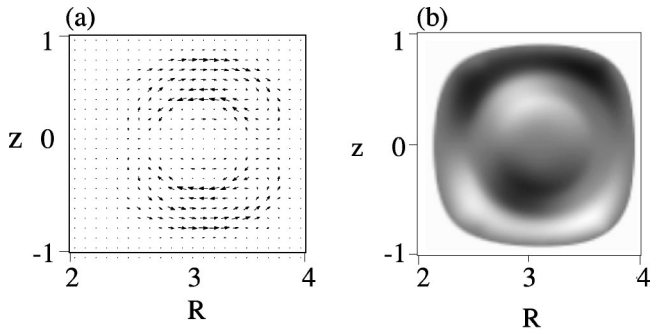

FIG. 3. Self-consistent axisymmetric flow. The (a) poloidal and (b) toroidal components of the axisymmetric flow $\langle \mathbf{V} \rangle_\phi$ at $t=1100\tau_A$ are plotted in the poloidal plane (R,z).

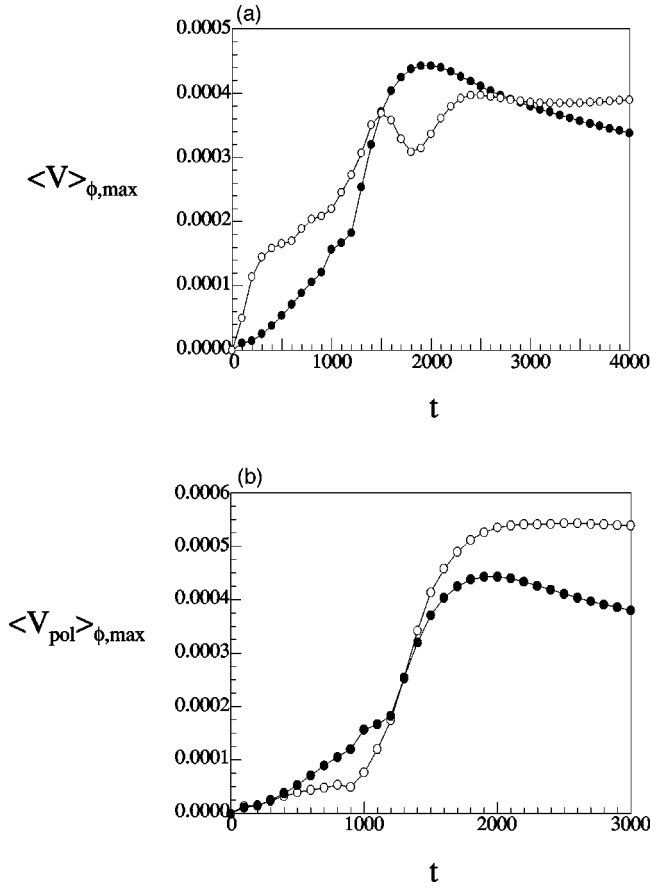

FIG. 4. Temporal variation of the axisymmetric flow. The temporal dependence of the maximum value of the poloidal flow (solid circles) and toroidal flow (open circles) when $\eta=\mu=3\times10^{-4}$ is plotted in (a). The plot in (b) is a comparison of the poloidal flow when $\eta=\mu=3\times10^{-4}$ (closed circles) with the poloidal flow when $\eta=\mu=2\times10^{-4}$ (open circles).

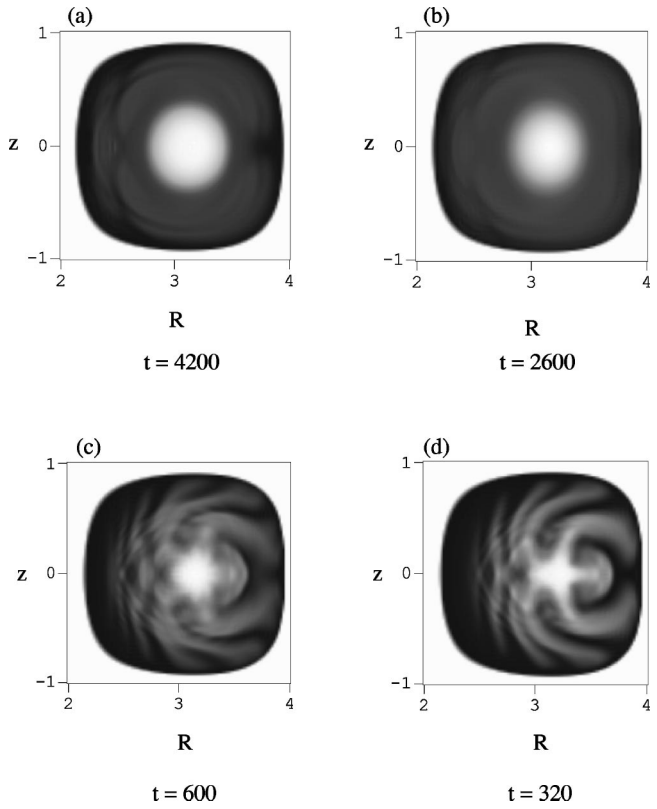

FIG. 5. Pressure evolution with increasing β. The pressure is plotted in the poloidal plane (R,z) for a tokamak plasma with β_{pol}=(a) 0.1, (b) 0.5, (c) 0.7, and (d) 1.0.

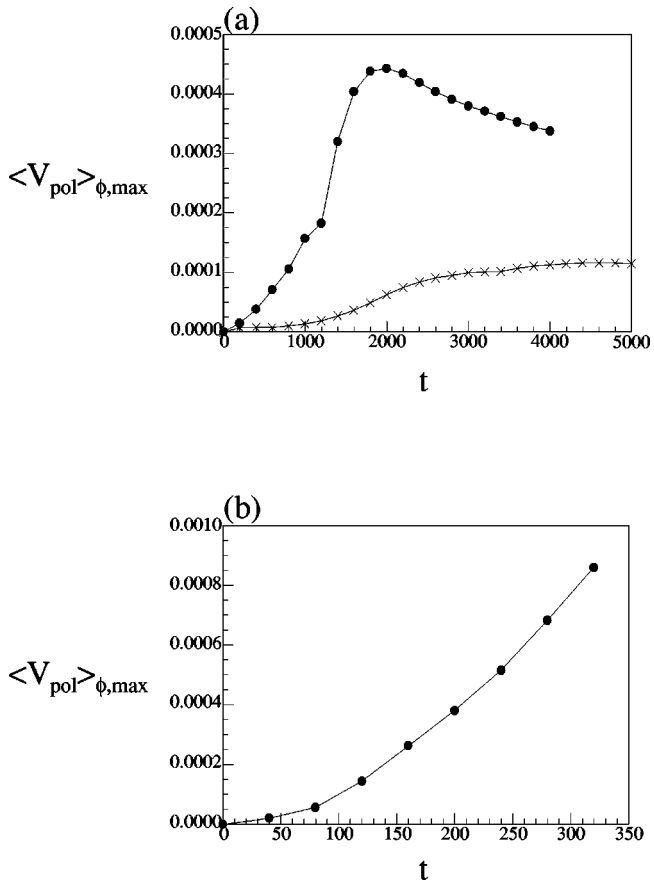

FIG. 6. Axisymmetric flow with increasing β. The temporal dependence of the maximum value of the poloidal axisymmetric flow is plotted for (a) $\beta_{\mathrm{pol}}=0.1$ (crosses) and $\beta_{\mathrm{pol}}=0.3$ (circles), and (b) $\beta_{\mathrm{pol}}=1$.

simulation shown in Figs. 2–4(a) is much larger than the dissipation at the center of a large, hot tokamak. However, the magnitude of the self-generated axisymmetric flow does not decrease as the dissipation is reduced in magnitude. Figure 4(b) is comparison of the temporal evolution of the axisymmetric poloidal flow for two different values of the dissipation, $\eta=\mu=3\times10^{-4}$ (solid circles) and $\eta=\mu=2\times10^{-4}$ (open circles). When the dissipation is reduced to $\eta=\mu=2\times10^{-4}$, the growth of the fingers is blunted by a self-generated flow in the same manner as shown in Figs. 2–4(a). In both cases there is a rapid rise in the axisymmetric flow from $t\sim1000\tau_A$ to $t\sim1500\tau_A$. The peak value of the flow does not decrease as the dissipation decreases, but actually increases slightly as the damping effect of the viscosity is reduced in magnitude.

IV. NONLINEAR STABILITY IN β

The results in Figs. 2–4 demonstrate that a linearly unstable $\beta_{\mathrm{pol}}=0.3$ tokamak equilibrium is nonlinearly stabilized by a self-consistently generated axisymmetric flow. We now consider the nonlinear stability of tokamak equilibria with increasing β. Figure 4 contains a series of plots that show the nonlinear states obtained for equilibria with β_{pol} from 0.1 to 1.

Like the $\beta_{\mathrm{pol}}=0.3$ equilibrium, a $\beta_{\mathrm{pol}}=0.1$ equilibrium is also nonlinearly stabilized by an axisymmetric flow [Fig. 5(a)]. But because the pressure gradient drive for the instabilities is weaker when $\beta_{\mathrm{pol}}=0.1$, the hot fingers grow more slowly and do not convect as far towards the wall at large R before their growth is blunted by the axisymmetric flow and the system relaxes into a stable quasiequilibrium. The hot central core of the plasma is unaffected. Figure 6(a) is a plot of the temporal evolution of the axisymmetric poloidal flow (crosses) during the nonlinear evolution of the perturbation when $\beta_{\mathrm{pol}}=0.1$. For the purpose of comparison, the axisymmetric poloidal flow for the $\beta_{\mathrm{pol}}=0.3$ toroidal plasma is also plotted (circles). The magnitude of the axisymmetric poloidal flow generated when $\beta_{\mathrm{pol}}=0.1$ is only $1\times10^{-4}v_A$, much smaller than when $\beta_{\mathrm{pol}}=0.3$. However, the small fingers of hot plasma grow so slowly that this small axisymmetric flow can act over a relatively long time and is very effective at halting the growth of the fingers before they become large. If the axisymmetric flow had not been effective at maintaining confinement, then the fingers would have grown larger and there would have been a larger transport of energy toward the wall at large R. Paradoxically, this greater broadening of the pressure profile would have generated an even larger axisymmetric flow. Thus, the very smallness of the axisymmetric flow is indicative of how effective the flow is at preventing the transport of energy toward the wall at large R, thereby maintaining the toroidal force balance.

As β_{pol} increases, the hot fingers grow more rapidly and convect ever more closely to the wall at large R before their progress is stopped. When $\beta_{\mathrm{pol}}=0.5$ [Fig. 5(b)], the hot fin-

FIG. 7. Three-dimensional structure. The figure shows a surface of constant pressure during the nonlinear evolution of the $\beta_{\mathrm{pol}}=1$ equilibrium, at $t=240\tau_A$.

gers almost reach the wall at large R, and the magnitude of the axisymmetric flow generated to finally stop them is more than 50% larger than when $\beta_{\mathrm{pol}}=0.3$. In this case, the central pressure decreases by about 10% as the pressure profile is broadened. As β_{pol} increases further, the fingers grow so rapidly that there is not sufficient time for the self-generated flow to stop them from reaching the wall. Although the hot fingers are deflected by the flow away from the wall toward the midplane when $\beta_{\mathrm{pol}}=0.7$ [Fig. 5(c)], the deflection is too small to prevent the fingers from barely striking the wall in about $600\tau_A$, and some of the energy in the plasma is lost.

At larger $\beta_{\mathrm{pol}}=1$ [Fig. 5(d)], the self-generated axisymmetric flow is even less effective. The axisymmetric poloidal flow shown in Fig. 6(b) rises to nearly $1\times10^{-3}v_A$ in only $320\tau_A$, about twice as large as the maximum axisymmetric poloidal flow generated when $\beta_{\mathrm{pol}}=0.3$. Although the axisymmetric flow is larger at higher β, the hot plasma fingers are convecting outward even more rapidly and there is insufficient time for the axisymmetric flow to halt the growth of the fingers before they strike the wall, leading to a global loss of confinement[4] in less than $320\tau_A$. With further increases in β_{pol}, the impact of the self-generated flow is negligible and the hot fingers directly strike the wall ever more rapidly. The three-dimensional structure of the pressure during the nonlinear growth of the fingers when $\beta_{\mathrm{pol}}=1$ is shown in Fig. 7. This figure is a plot of a surface of constant pressure at $t=240\tau_A$. This surface is characterized by a series of ridges and valleys that extend along the outside of the torus, where the local magnetic curvature is destabilizing. The fingers shown in Fig. 4(d) are the projection of these ridges and valleys onto the poloidal plane $\phi=0$.

V. SUMMARY

Our nonlinear toroidal MHD simulations demonstrate that the ultimate stability of tokamak plasmas is determined by nonlinear effects rather than by linear stability criteria. Linearly unstable equilibria at lower β do not suffer a disruptive loss of confinement because the linearly unstable modes are stabilized nonlinearly. As linearly unstable ballooning modes grow into the nonlinear phase, fingers of hot plasma start to convect out to the wall at large R. As the fingers grow, a self-consistent axisymmetric flow is generated nonlinearly, with both poloidal and toroidal components. This flow does not lie in a flux surface; the poloidal component is dominated by two vortices, one above the midplane of the torus and the other below. At lower β the fingers grow more slowly and the axisymmetric flow becomes large enough to halt the progress of the hot fingers before they reach the wall at large R. Although some of the energy is redistributed within the plasma, global confinement is maintained as the system relaxes into a stable quasiequilibrium containing flows. However, as β and the pressure gradient increase, the hot fingers grow more rapidly toward the wall. Although an axisymmetric flow is still generated, and is even larger in magnitude, when β becomes too large the growth of the fingers is so rapid that there is not sufficient time for the flow to grow large enough to halt the motion of the fingers before they strike the wall, and global confinement is lost. These simulations provide a natural explanation for the rapid loss of thermal confinement observed during disruptions on a time scale of the order of 100 μs, and not on longer time scales.[3] In the simulations, global confinement is lost only if the fingers grow rapidly enough to reach the wall in approximately 1000 τ_A (100 μs in a large tokamak). More slowly growing fingers are stabilized nonlinearly and do not lead to a loss of confinement. The simulations also provide a natural explanation for the variety of disruptions of varying intensity, from minor to major. Minor β disruptions in tokamaks are observed to be a less severe and somewhat slower manifestation of the instability responsible for major β disruptions.[3] Similarly, a small decrease in β in the simulations results in a decrease in the rate at which the fingers grow, and the self-generated flow reduces the impact of the fingers on confinement. Since the magnitude of the self-generated stabilizing flow in the simulations is only a few tenths of one percent of the sound speed, externally imposed flows of this magnitude may have an impact on tokamak stability.

When a nonlinear stability threshold in β is exceeded in our simulations, then there is a global loss of confinement as the hot plasma fingers grow rapidly enough to reach the wall before the self-consistently generated axisymmetric flow can stop them. Our simulations predict that the rapid loss of energy confinement observed during β limit disruptions is caused by coherent vortex flows that convect hot plasma fingers to the wall.[4] In contrast to the coherent fingers and vortex flows in our theory, Park *et al.*[6] claim that the loss of confinement during disruptions is caused by the generation of a stochastic magnetic field. Our view of the comparison between our theory of β limit disruptions and the theory of Park *et al.* is given in Refs. 4 and 7, while Park's view of the comparison is given in Ref. 8. In the present paper we have demonstrated, for the first time, that although a tokamak plasma is linearly unstable to ballooning modes, the plasma can still be nonlinearly stabilized by a self-generated axisymmetric flow, leading to a nonlinear stability limit in β.

[1]Y. Nagayama, M. Yamada, S. A. Sabbagh, E. D. Fredrickson, J. Manickam, M. Bell, R. V. Budny, A. Cavallo, A. C. Janos, M. E. Mauel, K. M. McGuire, G. A. Navratil, and G. Taylor, Phys. Fluids B **5**, 2571 (1993).
[2]M. Kikuchi and the JT-60 Team, in *Plasma Physics and Controlled-Nuclear Fusion Research* 1994, in *Proceedings of the 15th International Conference, Seville* (International Atomic Energy Agency, Vienna, 1995), Vol. I, p. 31.
[3]E. D. Fredrickson, K. McGuire, Z. Chang, A. Janos, M. Bell, R. V. Budny, C. E. Bush, J. Manickam, H. Mynick, R. Nazikian, and G. Taylor, Phys. Plasmas **2**, 4216 (1995).
[4]R. G. Kleva and P. N. Guzdar, Phys. Rev. Lett. **80**, 3081 (1998).
[5]R. G. Kleva and P. N. Guzdar, Phys. Plasmas **6**, 116 (1999).
[6]W. Park, E. D. Fredrickson, A. Janos, J. Manickam, and W. M. Tang, Phys. Rev. Lett. **75**, 1763 (1995).
[7]R. G. Kleva and P. N. Guzdar, Phys. Rev. Lett. **82**, 5414 (1999).
[8]W. Park and E. D. Fredrickson, Phys. Rev. Lett. **82**, 5413 (1999).